Supporting Information for:

Spin-state dependence of the structural and vibrational properties of solvated iron(II) polypyridyl complexes from AIMD simulations: aqueous [Fe(bpy)$_3$]Cl$_2$, a case study

Latévi M. Lawson Daku

Département de chimie physique, Université de Genève, Quai E. Ansermet 30, CH-1211 Genève 4, Switzerland. E-mail: max.lawson@unige.ch

Contents

List of Figures

List of Tables

1 Low-lying states of polypyridyl Fe(II) complexes
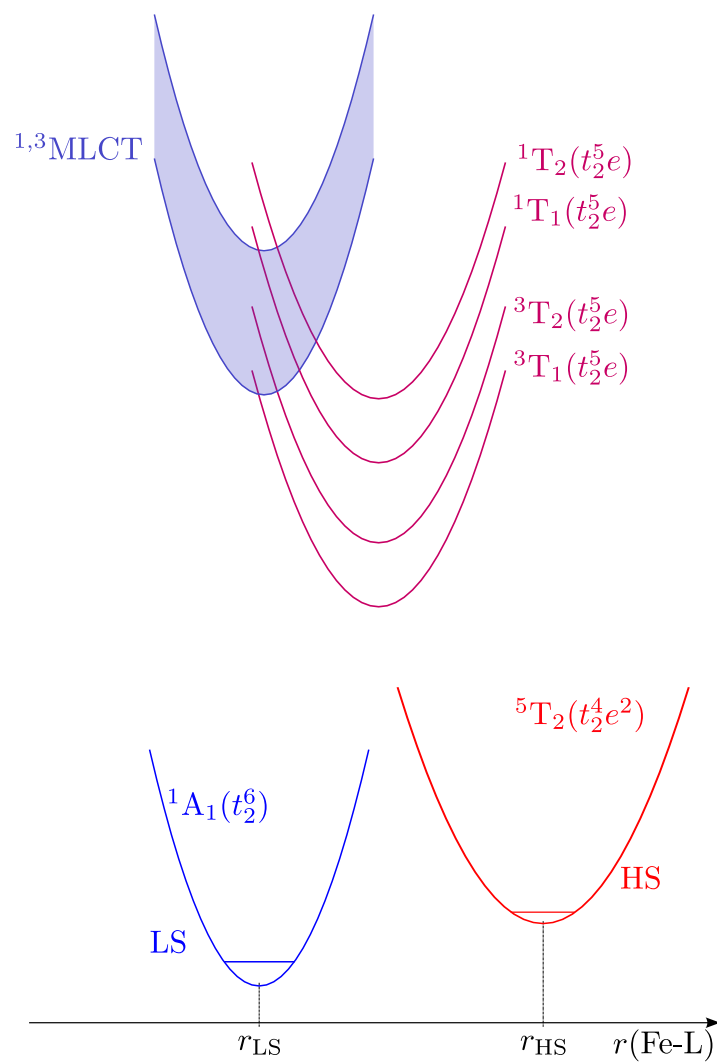

Figure S1 Low-lying states of polypyridyl Fe(II) complexes: schematic representation of the sections of the potential energy surfaces along the average metal-ligand distance coordinate.

2 Structural properties of the solution

2.1 The structure of the solvent
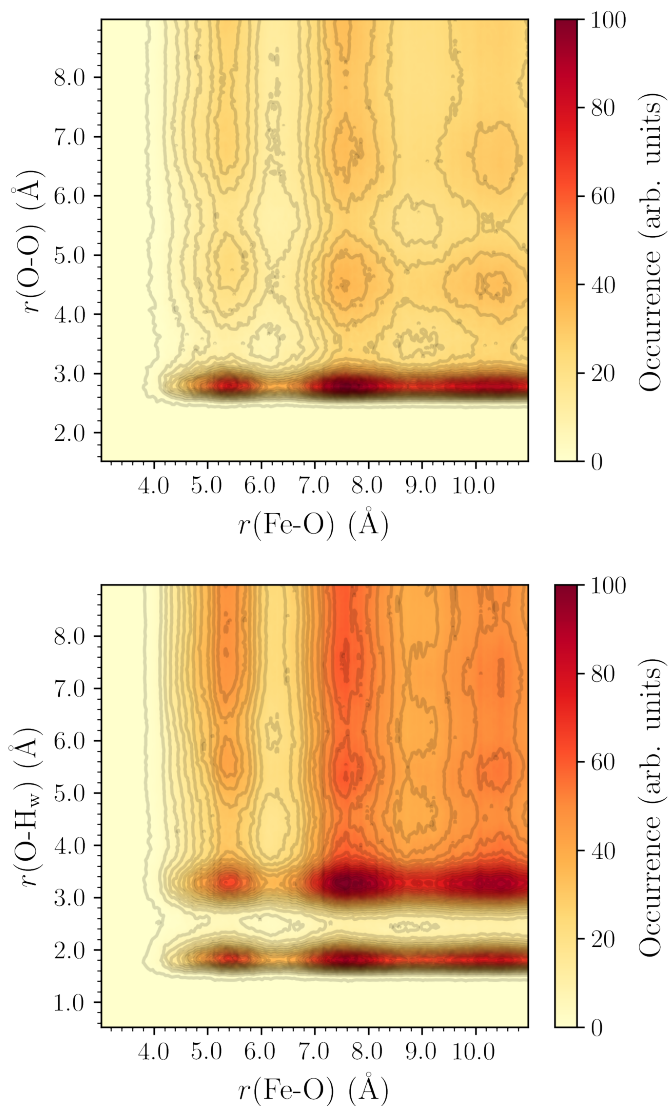
Figure S2 Combined Fe-O/O-O (top) and Fe-O/O-H$_\mathrm{w}$ (bottom) radial/radial distribution functions for aqueous [Fe(bpy)$_3$]$^{2+}$ in the HS state.

2.2 Solvation structure of the Cl$^-$ anions

For the $g_{\mathrm{ClH_w}}(r)$ or $g_{\mathrm{ClO_w}}(r)$ radial distribution functions, small differences are observed between the LS and HS curves beyond the radii of the minima associated to the first hydration

shell of Cl^-. They are not necessarily due to the influence of the spin state of $[Fe(bpy)_3]^{2+}$ but more likely to the finite durations of the simulations, which do not suffice to completely average out the variances between the trajectories of the anions. As illustrated by the plots in Figure S3 of the Fe-Cl distances as functions of time, there are indeed marked differences between the trajectories of the anions. One notes in particular that a Cl^- anion enters the first solvation shell of $[Fe(bpy)_3]^{2+}$ in the LS state. Still, (i) the resulting differences between the LS and HS $g_{ClH_w}(r)$ or $g_{ClO_w}(r)$ RDFs are small and for the description of the outer coordination spheres of Cl^-, and (ii) the calculated RDFs compare well with experiments.
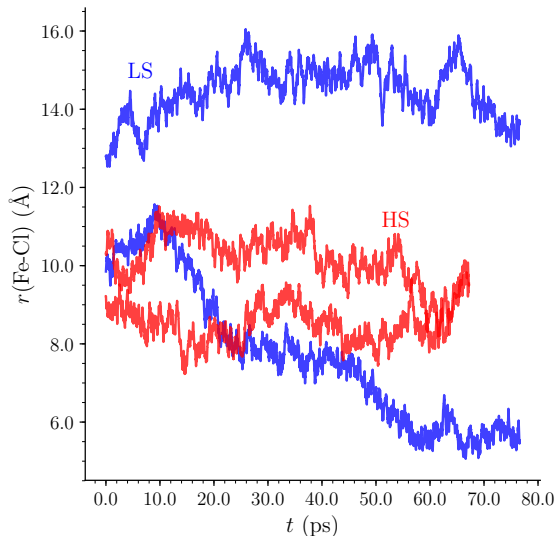

Figure S3 Time dependence of the Fe-Cl distances for $[Fe(bpy)_3]^{2+}$ in the LS and in the HS state.

The pairing which is taking place between a Cl^- ion and $[Fe(bpy)_3]^{2+}$ in the LS state can also happen for the complex in the HS state. However, the occurrence of such an event is expected to be relatively weak given the low concentration of $0.179\,mol/L$ of the $[Fe(bpy)_3](Cl)_2$ solution. Investigating the ion pairing in the aqueous solution would necessitate very long simulation times, which is computationally not affordable in the framework of the present AIMD study. The observed contact did not lead to peculiar features in the calculated RDFs and CDFs describing the solvation structure of LS $[Fe(bpy)_3]^{2+}$. Furthermore, as shown in Ref. 1, Cl^- ions are readily accommodated into the H-bond network of water, substituting an oxygen site with no major changes to the water network. Consequently, the local per-

turbations to the hydration structure of $[Fe(bpy)_3]^{2+}$ brought by $Cl^- - [Fe(bpy)_3]^{2+}$ pairing are expected to only have a minor influence on the organization of the solvent around the complex, and thus to not significantly alter the description achieved in the present study for the hydration structure of $[Fe(bpy)_3]^{2+}$ in the two spin states.

3 Dipole moments

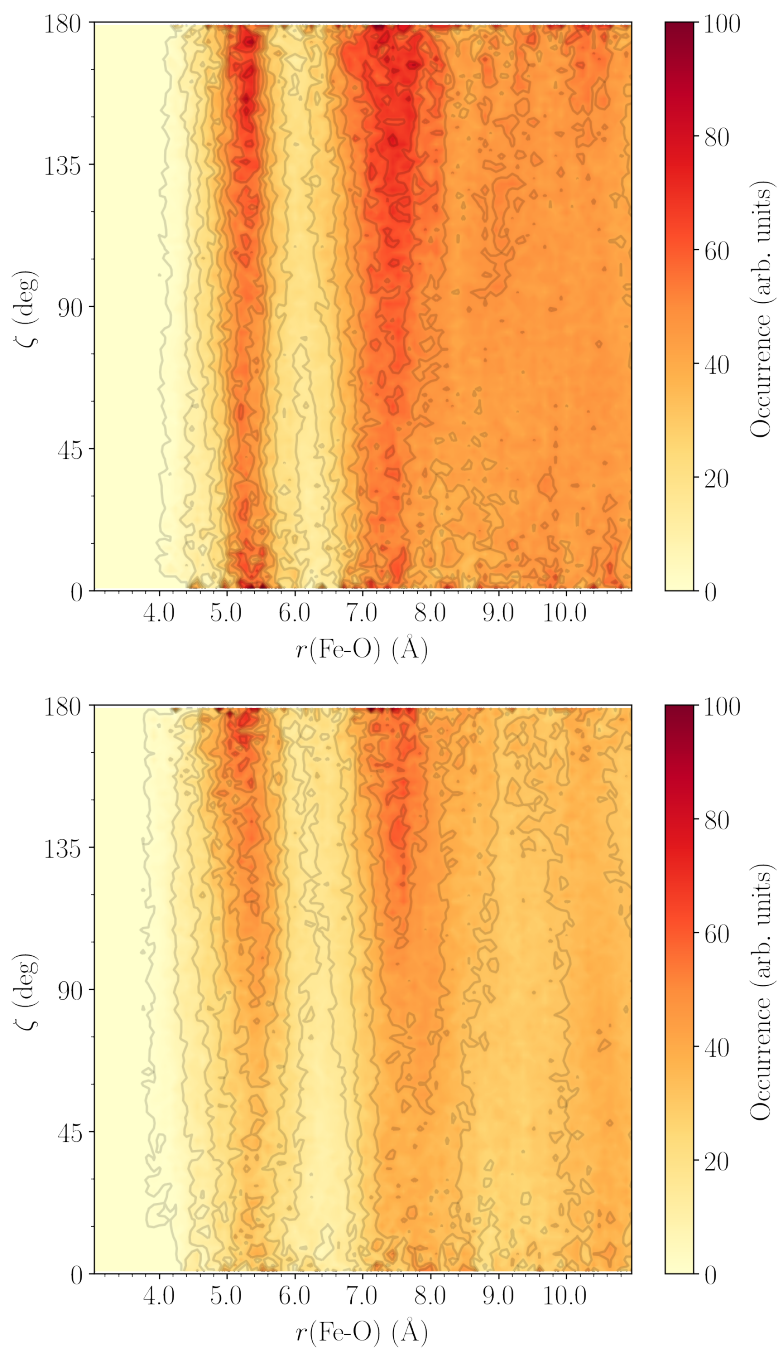## 3.1 Combined Fe-O/ζ radial/angular distribution functions

Figure S4 Combined Fe-O/ζ radial/angular distribution function for $[Fe(bpy)_3]^{2+}$ in the LS (Top) and in the HS (Bottom) state (ζ: angle between the dipole moment of $[Fe(bpy)_3]^{2+}$ and that of the observed water molecule).

4 Vibrational properties

4.1 Vibrational densities of states of aqueous HS $[Fe(bpy)_3]^{2+}$

The total and 177 mode-specific VDOS determined for aqueous HS $[Fe(bpy)_3]^{2+}$ are plotted over the $0-3500$ cm^{-1} range in Figure S5. The sharp peak at $\bar{\nu} \approx 3200$ cm^{-1} is the sum of the VDOS of the 24 CH stretching modes (Figure S5d, modes $154-177$), while the contributions to the total VDOS in the fingerprint region (Figure S5c) originate from 108 ligand-centered vibrational modes (modes $46-153$), which are the CC and CN stretching or torsion modes, the in-plane or out-of-plane CH bending modes, or the in-plane ring bending modes. As for the total VDOS in the far-IR region, the modes $1-45$ contribute to this region, and their VDOS extend into the mid-IR region (Figure S5b). These low-energy vibrations correspond to librations of the ligands or of their pyridyl moieties, to out-of-plane ring bending modes, and to vibrations centered on the Fe-N bonds.
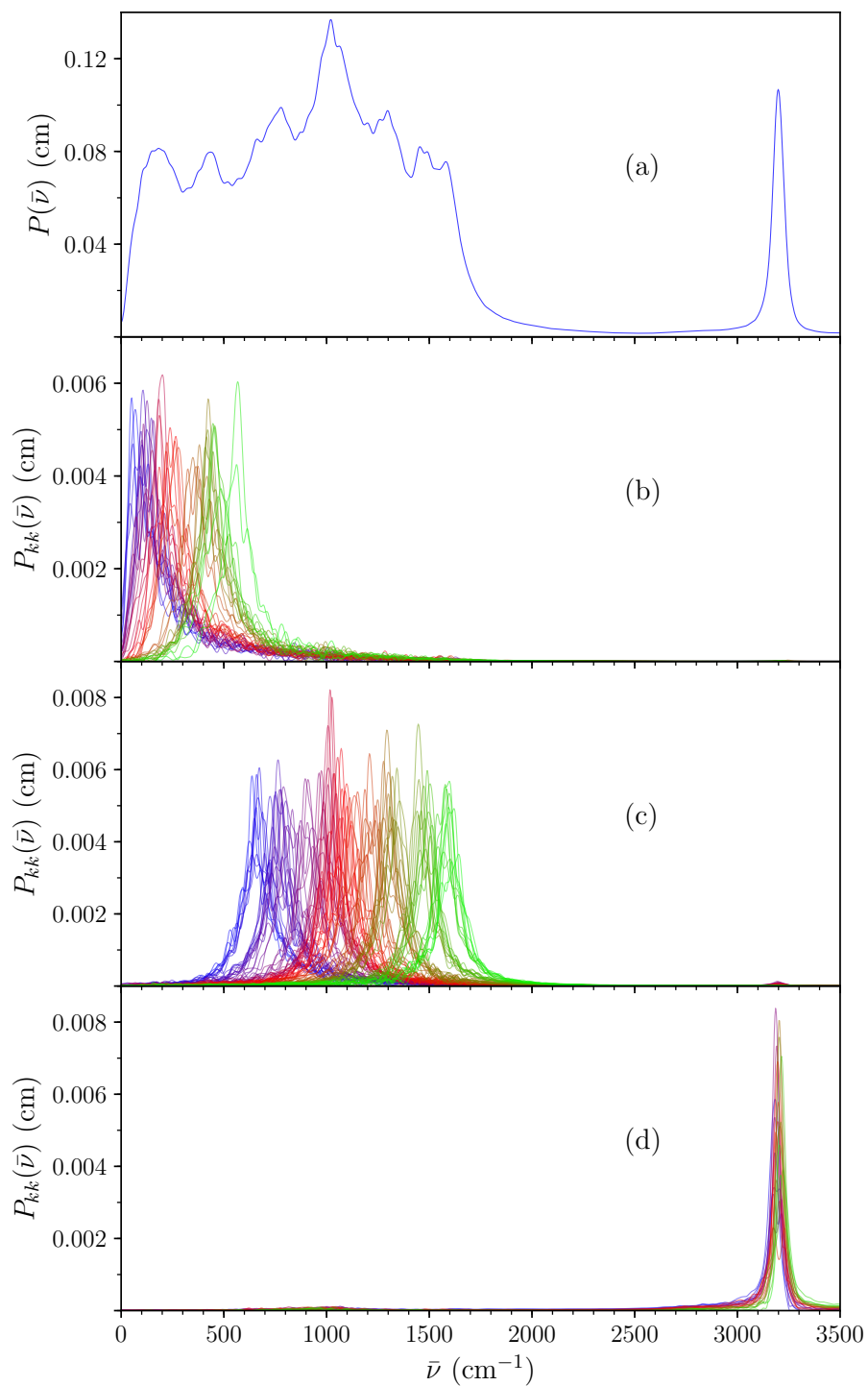
Figure S5 Generalized normal coordinate analysis for aqueous HS [Fe(bpy)$_3$]$^{2+}$ at 310 K (resolution of the ACFs: 512 time steps): (a) total vibrational density of states (VDOS) and mode–specific VDOS located in (b) the far IR region (modes 1−45), (c) the fingerprint region (modes 46−153), and (d) in the CH stretch region (modes 154−177).

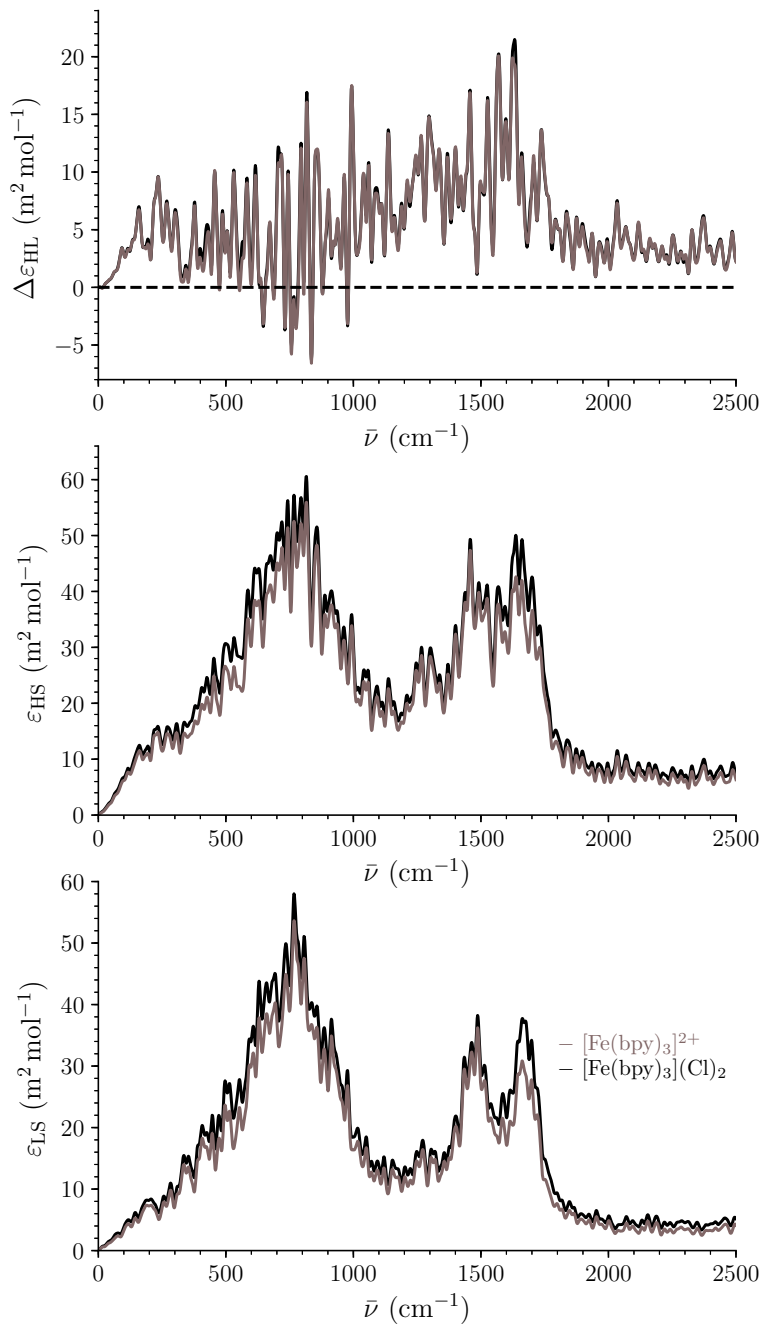## 4.2 Comparison between the IR spectra of aqueous $[Fe(bpy)_3](Cl)_2$ and aqueous $[Fe(bpy)_3]^{2+}$

Figure S6 Comparison between the calculated 310 K LS (bottom) and HS (middle) IR spectra of aqueous $[Fe(bpy)_3](Cl)_2$ and aqueous $[Fe(bpy)_3]^{2+}$, and between the corresponding HS-LS difference curves (top; resolution of the ACFs: 512 time steps).

4.3   IR spectrum of water
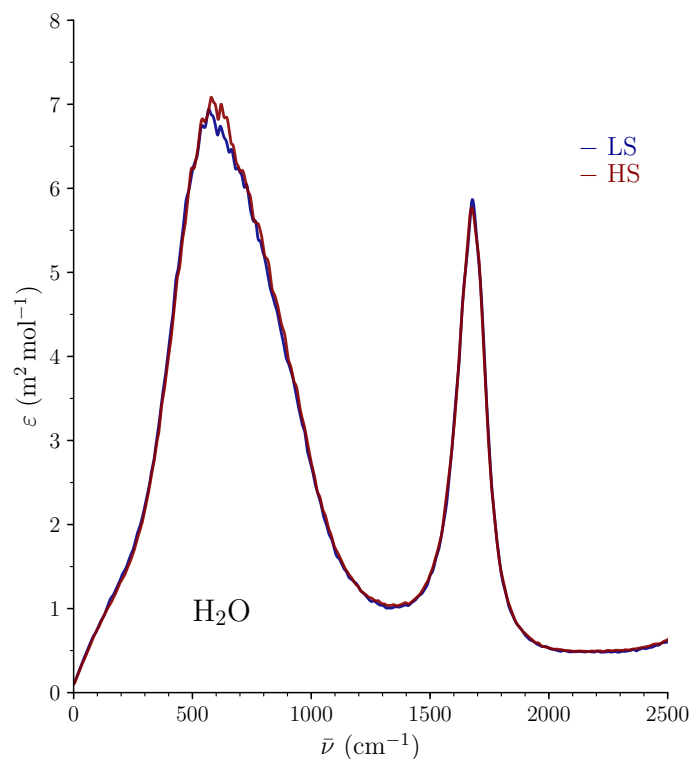
Figure S7 Calculated 310 K IR spectra of water in the 0-2500 cm^{-1} range for the aqueous solution of [Fe(bpy)$_3$](Cl)$_2$ in the LS and HS states (resolution of the ACFs: 512 time steps). The calculated spectra are in good agreement with experiments[2,3] and with recent theoretical results.[4–7] The low-energy broad band encompasses the bands due to the libration of the water molecules at ~380 cm^{-1} (L$_1$ band) and ~670 cm^{-1} (L$_2$ band), as well as the contributions from the bending and stretching modes of the hydrogen bonds at 50~60 cm^{-1} and ~180 cm^{-1}, respectively. The band at 1675 cm^{-1} corresponds to the bending mode of the water molecules.

4.4 Selected generalized normal coordinates of aqueous [Fe(bpy)$_3$]$^{2+}$

Table S1 Generalized normal coordinate analysis for aqueous [Fe(bpy)$_3$]$^{2+}$ in the LS state (resolution of the ACFs: 512 time steps): vibration modes involving the Fe-N bonds

$k = 14$

$k = 15$

$k = 16$

$k = 17$
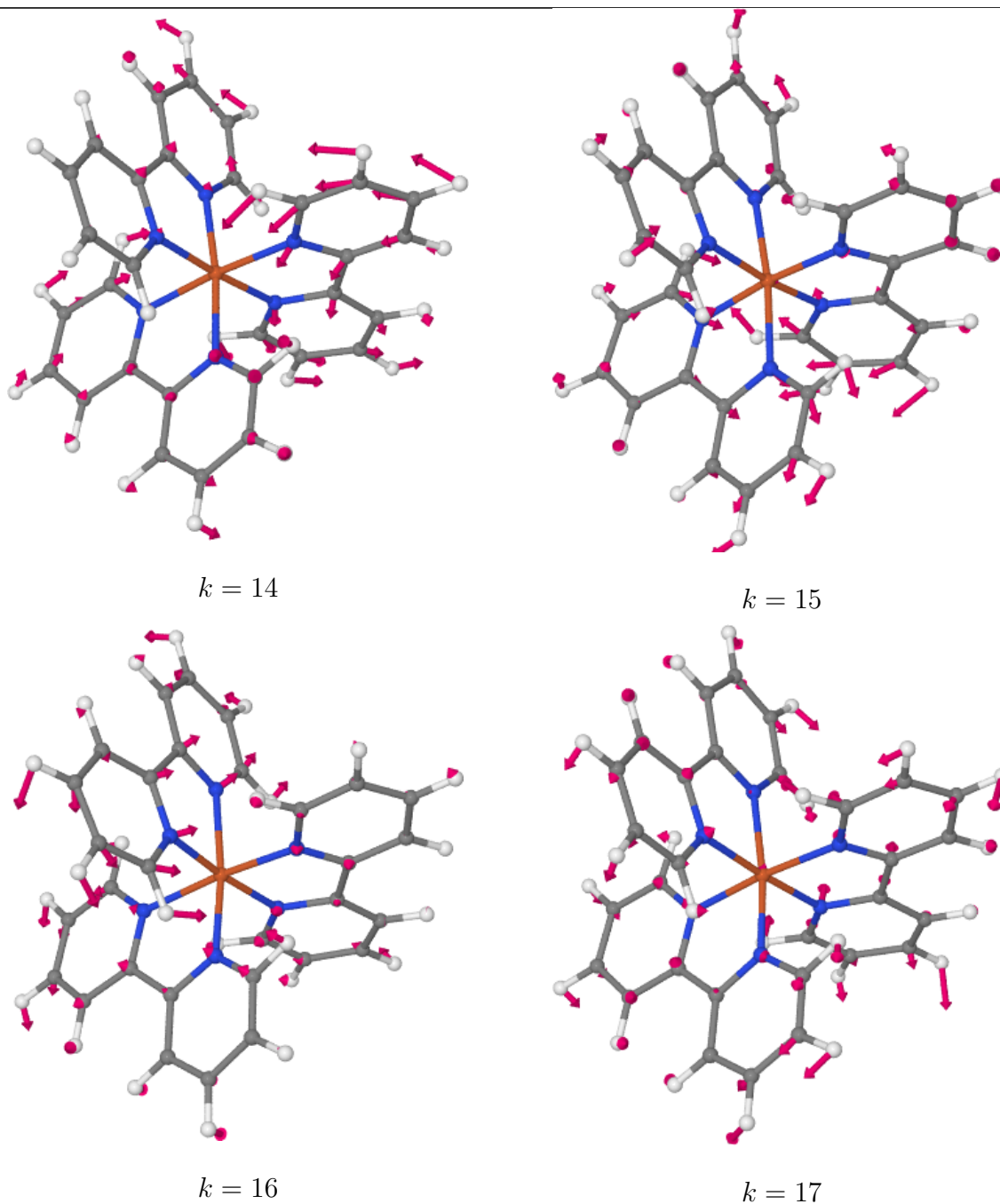
Continued next page.
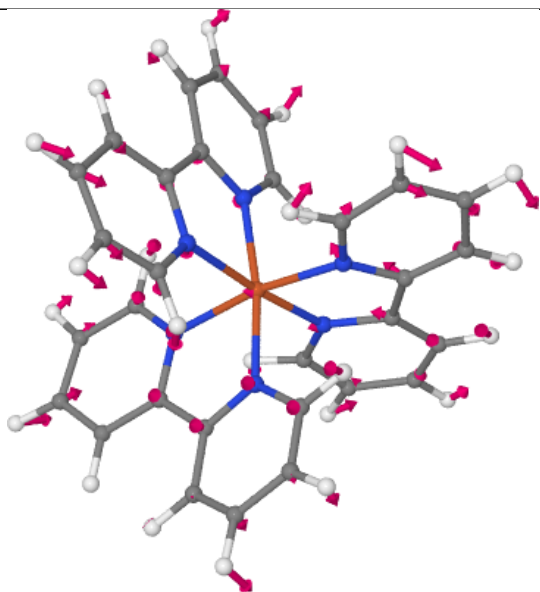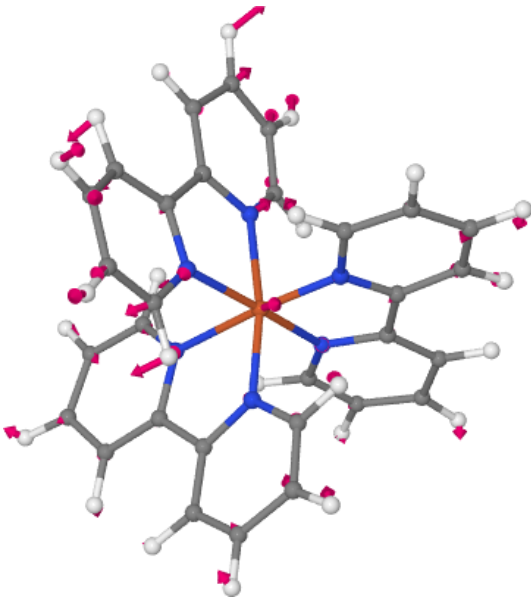
$k = 18$
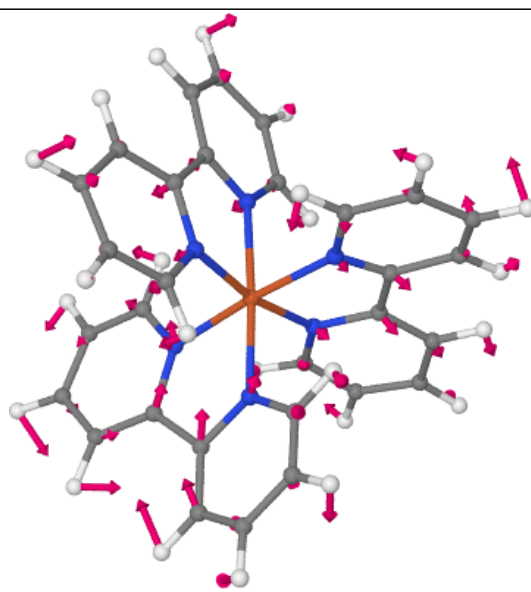
$k = 19$
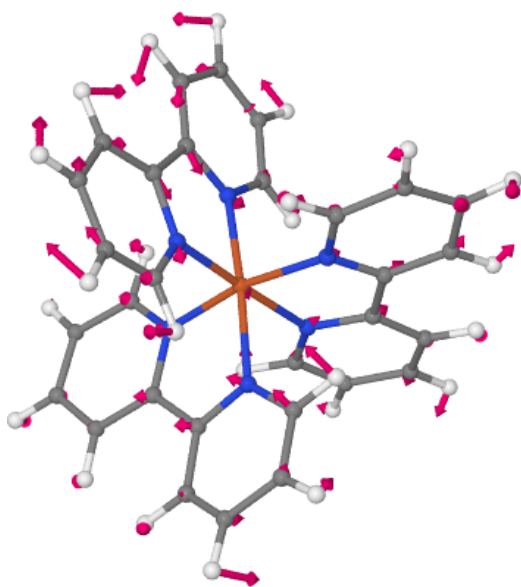
$k = 20$
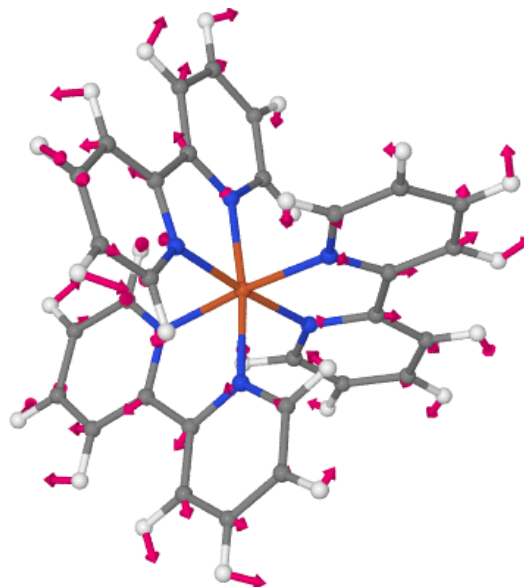
$k = 21$

Continued next page.
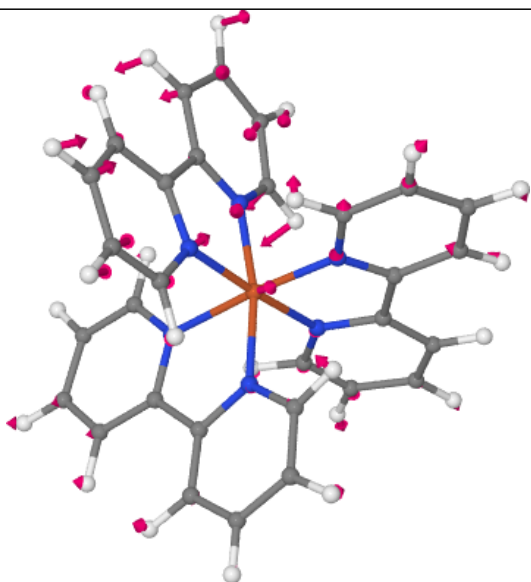
$k = 25$
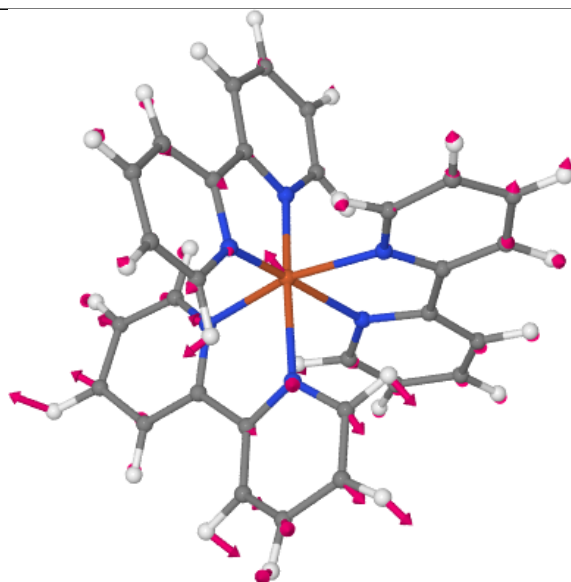
$k = 26$
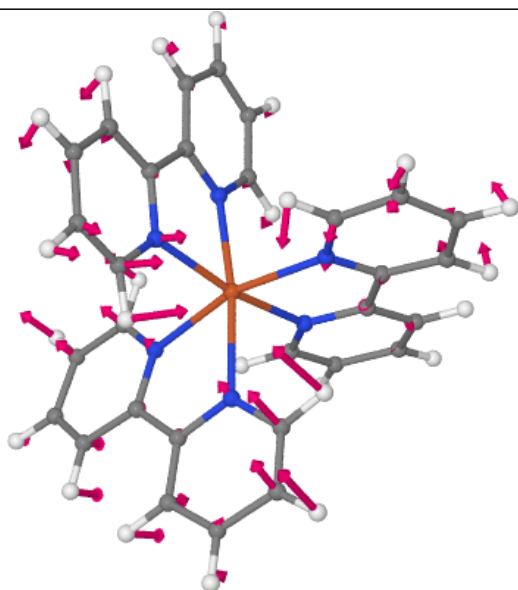
$k = 27$
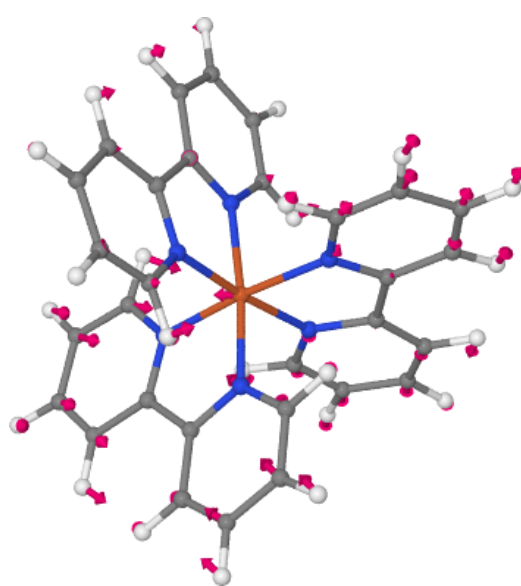
$k = 28$

Continued next page.
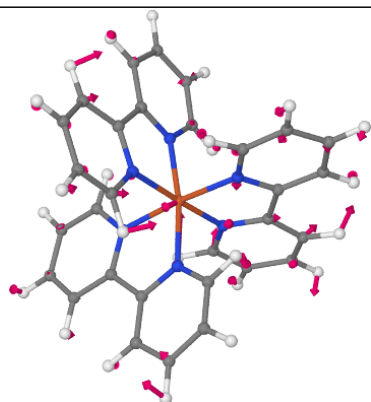
$k = 29$
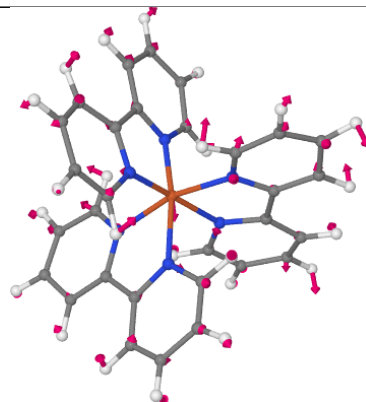
$k = 30$

Table S2 Generalized normal coordinate analysis for aqueous $[\text{Fe(bpy)}_3]^{2+}$ in the HS state (resolution of the ACFs: 512 time steps): vibration modes involving the Fe-N bonds
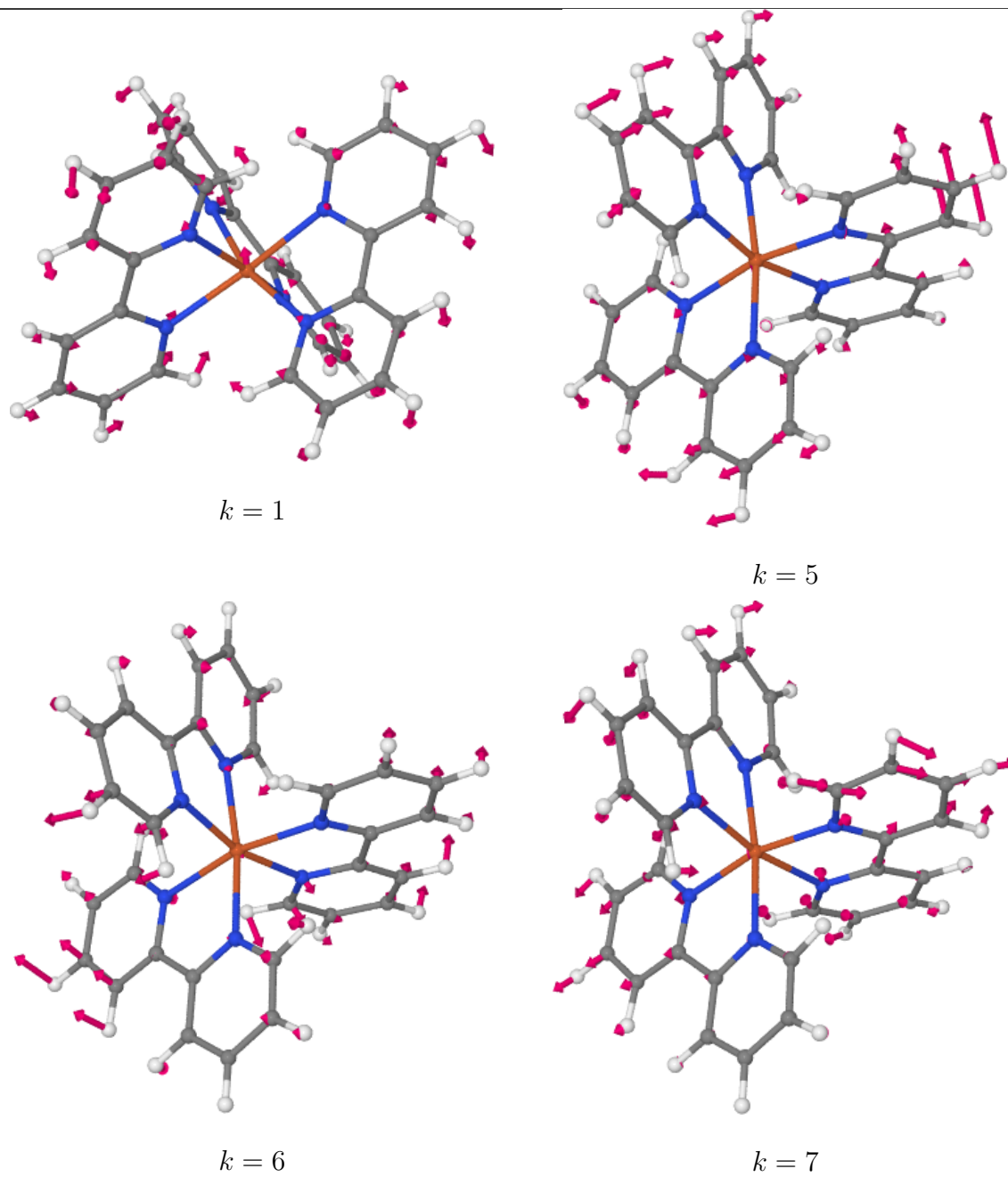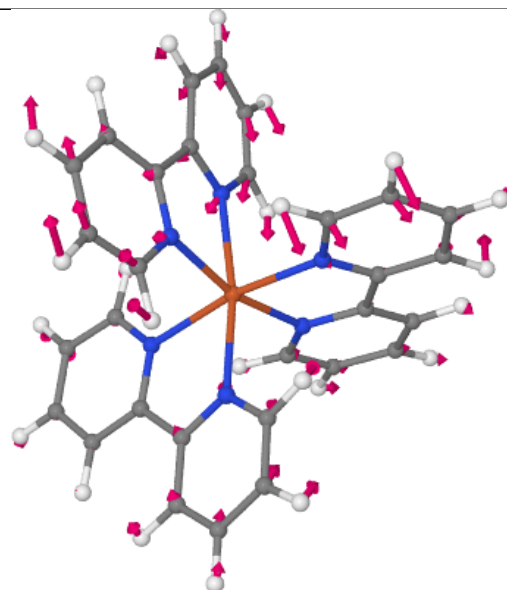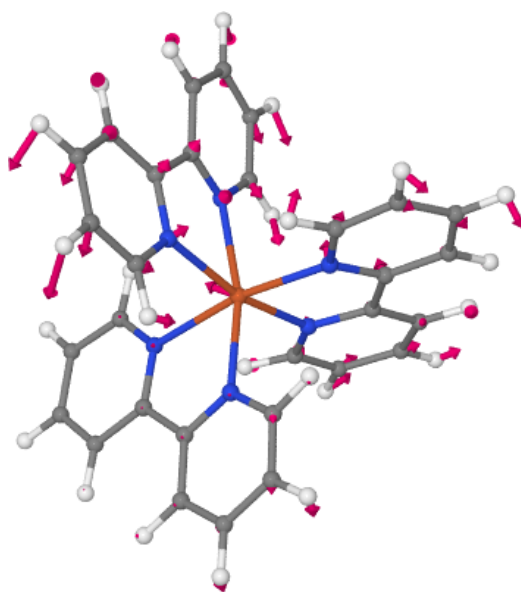

$k = 1$

$k = 5$

$k = 6$

$k = 7$

Continued next page.

$k = 8$

$k = 10$

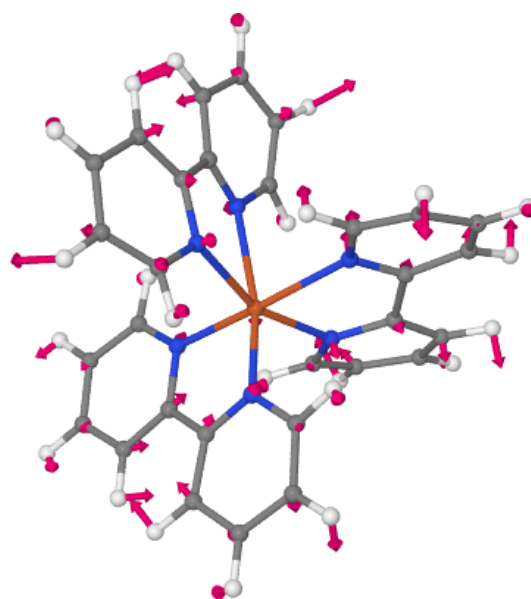$k = 17$

$k = 19$
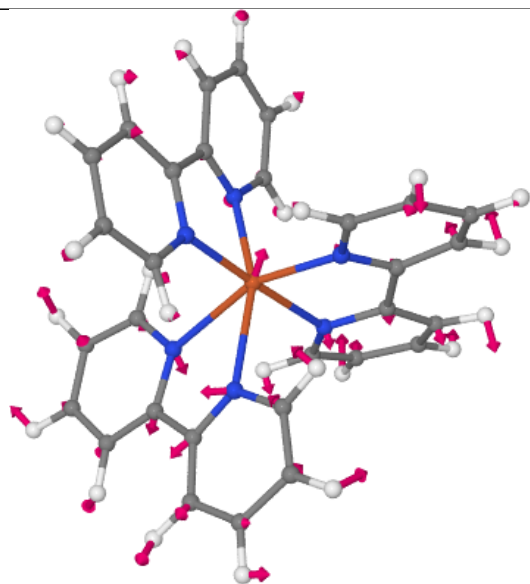
19
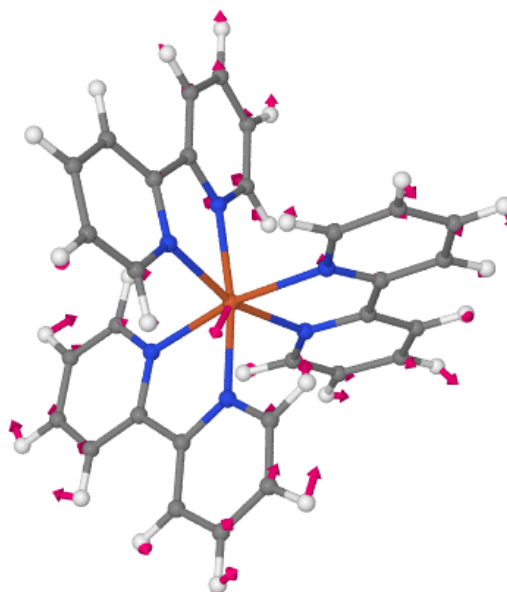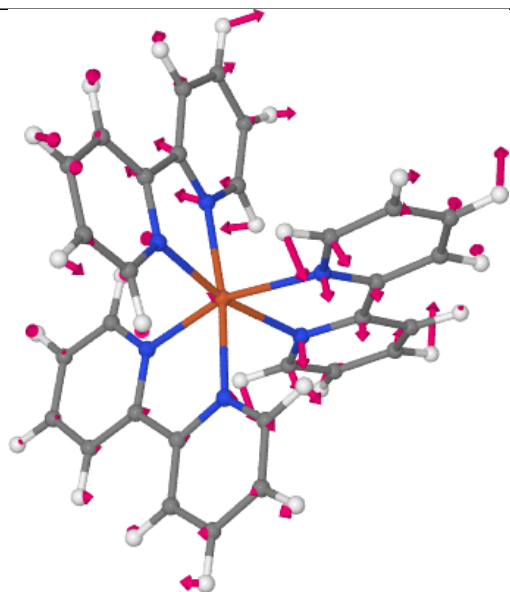
$k = 20$
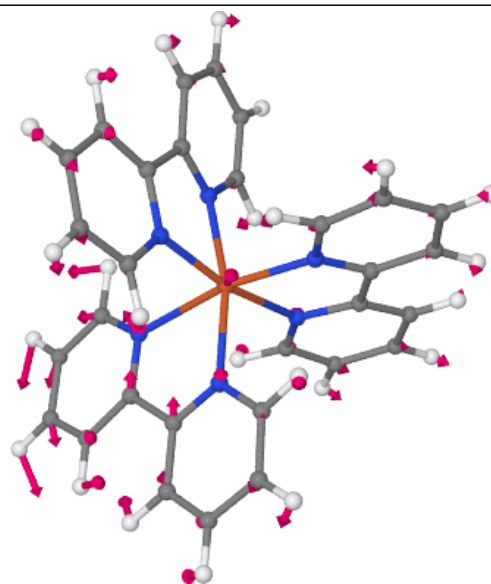
$k = 21$
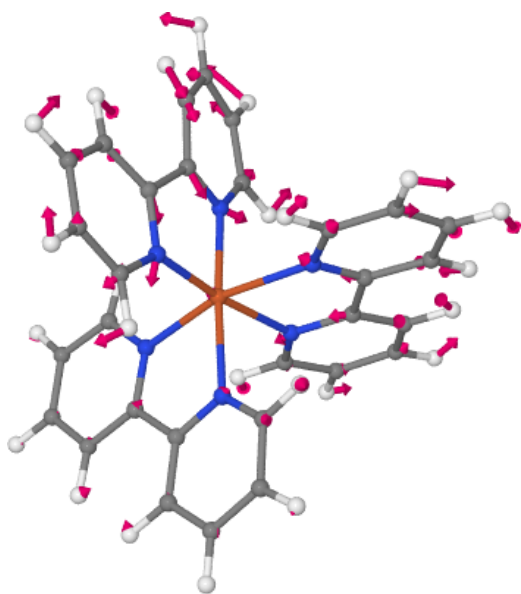
$k = 22$
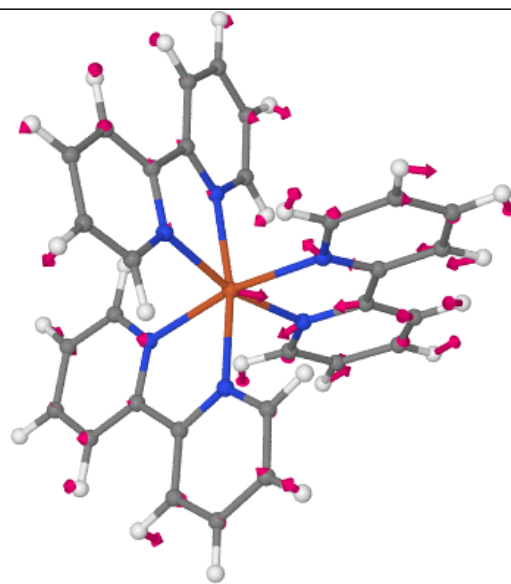

$k = 23$

Continued next page.

20

$k = 24$ $k = 26$

References

1 R. Mancinelli, A. Botti, F. Bruni, M. A. Ricci and A. K. Soper, *J. Phys. Chem. B*, 2007, **111**, 13570–13577.

2 H. R. Zelsmann, *J. Mol. Struct.*, 1995, **350**, 95 – 114.

3 J. E. Bertie and Z. Lan, *Appl. Spectrosc.*, 1996, **50**, 1047–1057.

4 M. Sharma, R. Resta and R. Car, *Phys. Rev. Lett.*, 2005, **95**, 187401.

5 G. R. Medders and F. Paesani, *J. Chem. Theory Comput.*, 2015, **11**, 1145–1154.

6 H. Liu, Y. Wang and J. M. Bowman, *J. Phys. Chem. B*, 2016, **120**, 1735–1742.

7 http://www1.lsbu.ac.uk/water/water_vibrational_spectrum.html (Last accessed: November 2, 2017).